Effect of operational conditions on sonoluminescence and kinetics of H2O2 formation during the sonolysis of water in the presence of Ar/O2 gas mixture

ARTICLE *in* ULTRASONICS SONOCHEMISTRY · FEBRUARY 2015

Impact Factor: 4.32 · DOI: 10.1016/j.ultsonch.2015.02.005 · Source: PubMed

5 AUTHORS, INCLUDING:

Rachel Pflieger
Institut de Chimie Séparative de Marcoule
31 PUBLICATIONS **188** CITATIONS
SEE PROFILE

Tony Chave
Institut de Chimie Séparative de Marcoule
31 PUBLICATIONS **392** CITATIONS
SEE PROFILE

Sergey Nikitenko
Atomic Energy and Alternative Energies Co…
79 PUBLICATIONS **1,217** CITATIONS
SEE PROFILE

Ultrasonics Sonochemistry 26 (2015) 169–175

Contents lists available at ScienceDirect

Ultrasonics Sonochemistry

journal homepage: www.elsevier.com/locate/ultson

Effect of operational conditions on sonoluminescence and kinetics of H_2O_2 formation during the sonolysis of water in the presence of Ar/O_2 gas mixture

Rachel Pflieger, Tony Chave, Ghislain Vite, Lucie Jouve, Sergey I. Nikitenko *

Institut de Chimie Séparative de Marcoule (ICSM), UMR 5257 – CEA – CNRS – UMII – ENSCM, Centre de Marcoule, BP 17171, 30207 Bagnols-sur-Cèze Cedex, France

ARTICLE INFO

Article history:
Received 22 September 2014
Received in revised form 26 January 2015
Accepted 9 February 2015
Available online 14 February 2015

Keywords:
Sonochemistry
Ultrasound
Sonoluminescence
Oxygen
Degassing
Hydrogen peroxide

ABSTRACT

Ultrasonic frequency is a key parameter determining multibubble sonoluminescence (MBSL) spectra of water saturated with Ar/O_2 gas mixtures. At 20 kHz, the MBSL is quenched by oxygen. By contrast, at high-frequency ultrasound the maximal MBSL intensity is observed in the presence of $Ar/20\%O_2$ gas mixture. Nevertheless, oxygen has no influence on the shape of MBSL spectra. The effect of oxygen on MBSL is explained by oxygen dissociation inside the collapsing bubble which is much more effective at high ultrasonic frequency compared to 20 kHz ultrasound. In contrast to MBSL, a higher yield of H_2O_2 is observed in $Ar/20\%O_2$ gas mixture whatever the ultrasonic frequency. At 20 °C and 20% of oxygen the maximal yield of H_2O_2 is observed at 204–362 kHz. The maximal yield of H_2O_2 is shifted to 613 kHz when the bulk temperature is raised up to 40 °C. Coupling of high-frequency ultrasound with mechanical stirring and intensive Ar/O_2 bubbling improves H_2O_2 production. Comparison of MBSL and sonochemistry allowed to conclude that H_2O_2 is formed from non-excited $OH^{\cdot}$ ($X^2\Pi$) and $HO_2^{\cdot}$ radicals. Finally, it was shown that at the studied conditions the efficiency of ultrasonic degassing is hardly influenced by frequency.

1. Introduction

Over the past few decades, sonochemistry in aqueous solutions has been extensively studied as an advanced oxidation process (AOP) potentially suitable for waste water treatment [1–9]. The sonochemical AOP is based on the generation of oxidative species during acoustic cavitation in water, particularly $OH^{\cdot}$ and $HO_2^{\cdot}$ radicals and hydrogen peroxide H_2O_2 formed as a secondary product of radical recombination. The efficiency of oxidizing species production is affected by a number of factors including ultrasonic frequency, acoustic power, sparge gas, external pressure and solution temperature. Several authors have reported higher H_2O_2 formation rate in argon-saturated water at high-frequency ultrasound (>100 kHz) compared to low-frequency 20 kHz ultrasound [10–14]. The yield of H_2O_2 ($G_{H_2O_2}$) is strongly increased in the presence of oxygen, which was attributed to much more significant generation of both $OH^{\cdot}$ and $HO_2^{\cdot}$ radicals [5,10,12,15]. With a gas mixture of 80–70% argon and 20–30% oxygen, the $G_{H_2O_2}$ value was found to be drastically higher than for water sonication under pure argon or pure oxygen whatever the ultrasonic frequency [15]. At higher oxygen concentration $G_{H_2O_2}$ decreases, which has been attributed to the drop of intrabubble temperature in the presence of a polyatomic gas presuming adiabatic heating during bubble collapse [15,16]. However, the influence of ultrasonic frequency on the sonochemical reactions with oxygen is as yet poorly understood. For example, Henglein et al. [16] have shown that at high ultrasonic frequency (300 kHz) oxygen molecules may dissociate inside the cavitation bubble. By contrast, these processes have never been reported for low-frequency ultrasound. Recent studies revealed that the variation of ultrasonic frequency, in particular between low and high frequencies, could lead not only to a change in reaction kinetics but also to significant modifications of reaction mechanisms [13].

Spectroscopic studies of sonoluminescence provide a powerful tool to better understand sonochemical mechanisms. However, the relationship between sonochemical activity and sonoluminescence has just begun to emerge. Usually, the sonochemical activity is compared with the total intensity of sonoluminescence or with the intensity of chemiluminescence produced in sonicated solutions of luminol [12,17]. It should be emphasized that the multibubble sonoluminescence (MBSL) spectra in water are quite complex and contain emission lines attributed to different electronic and vibrational excited states of $OH^{\cdot}$ radicals and H_2O molecules [18,19]. The variation of the experimental parameters could generate the redistribution of relative line intensities and

* Corresponding author. Tel.: +33 466339251.
E-mail address: serguei.nikitenko@cea.fr (S.I. Nikitenko).

http://dx.doi.org/10.1016/j.ultsonch.2015.02.005
1350-4177/

not only a change in total emission intensity. Therefore, a thorough spectroscopic analysis of MBSL spectra is required to elucidate the impact of experimental conditions on reaction mechanism. This paper describes a comparative study of H_2O_2 formation rate and MBSL spectra in water saturated with Ar/O_2 gas mixtures at different ultrasonic frequencies.

2. Materials and methods

2.1. Materials

Deionized water (Milli-Q 18.2 MΩ cm) was used to prepare all aqueous solutions. Argon and oxygen at 99.999% purity and 20%O_2/Ar gas mixture were provided by Air Liquide. Reagents and chemicals used in the various procedures were all of analytical grade and were purchased from Sigma–Aldrich.

2.2. Reactor setup and MBSL measurements

The multifrequency ultrasonic device consisted of a thermostated glass-made batch reactor mounted on top of the high-frequency piezoelectric transducer (ELAC Nautik, 25 cm^2) providing 204–1057 kHz power ultrasound connected to a high-frequency generator with a maximum electrical power of 125 W (T & C Power Conversion, Inc.). Ultrasonic irradiation with low frequency ultrasound of 20 kHz was performed with 1 cm^2 titanium probe (750 W Sonics). The probe was placed reproducibly on top of the reactor opposite the high-frequency transducer using a tight Teflon ring. A new probe tip was used in each experiment to avoid the drop of SL due to the tip cavitation erosion. The absorbed acoustic power, P_{ac}, was measured by the conventional thermal probe method. At high ultrasonic frequency many experiments (not MBSL measurements) have been performed under additional mechanical stirring to provide a homogeneous temperature inside the reactor during the ultrasonic treatment. A glass-made three-bladed propeller agitator was then placed instead of the 20 kHz ultrasonic probe. Table 1 summarizes the values of acoustic power, P_{ac}, measured as a function of amplitude or electric load power, LP, for low- and high-frequency ultrasound.

For all experiments, 250 mL of the solutions were sparged with gas (Ar, O_2 or 20%O_2/Ar) about 30 min before sonication and during the ultrasonic treatment at a controlled rate of typically 80 mL min^{-1}. Gas flow rates were measured with a volumetric flowmeter with stainless steel float (Aalborg). The calibration chart provided by the manufacturer was validated against a numerical mass flowmeter (Aalborg GFM17). The temperature in the reactor during sonolysis was maintained with a Huber Unistat Tango thermo-cryostat and measured by a thermocouple immersed approximately 2 cm below the surface of the solution.

The light emission spectra were collected through a flat quartz window using parabolic Al-coated mirrors and recorded in the spectral range from 230 nm up to 600 nm using a SP 2356i Roper Scientific spectrometer (gratings 300blz300 and 150blz500, slit width 0.25 mm) coupled to a charge-coupled CCD camera with UV coating (SPEC10-100BR Roper Scientific) cooled by liquid-nitrogen. A high-pass filter was used when necessary to avoid second order light. Spectral calibration was performed using a Hg(Ar) pen-ray lamp (model LSP035, LOT-Oriel). The spectra acquisition was started after reaching a steady-state temperature. For each experiment, at least three 300 s spectra were averaged and corrected for background noise and for the quantum efficiencies of grating and CCD. The SL spectra were collected at the focusing point providing the highest light emission intensity without mechanical agitation.

Table 1
Values of acoustic power, P_{ac}, measured by thermal probe method for 20 kHz (a) and high-frequency ultrasound (b).

Amplitude, %[a]	Acoustic power, P_{ac} (W)	
(a)		
30	17	
40	24	
50	32	
60	40	
Frequency, kHz	Acoustic power, P_{ac} (W)	
	LP = 55 W[b]	LP = 73 W[b]
(b)		
204	32	41
362	43	57
613	43	57
1057	42	56

[a] Amplitude of the generator.
[b] Load electric power of the generator.

2.3. Analytical procedures

The concentration of dissolved oxygen was measured with Orion 3 Star meter (Thermo Scientific) after establishment of the steady state which was typically about 20 min. Hydrogen peroxide was monitored by absorption spectrophotometry with Ti(IV) in 0.5 M H_2SO_4 (λ = 411 nm, ε = 707 cm^{-1} M^{-1}). The statistical error for H_2O_2 formation rate was estimated to be 10%. Hydrogen in the outlet gas was analyzed using a Thermo Scientific VG Prolab Benchtop quadrupole mass spectrometer. The concentration of H_2 was followed with the multiple ion monitoring (MIM) provided by the software. The water vapor in the outlet gas was trapped using molecular sieves (Sigma–Aldrich, 3 Å) prior to mass spectrometric analysis.

3. Results and discussion

3.1. Effect of ultrasound on the concentration of dissolved oxygen

The steady-state concentration of dissolved oxygen, [O_2], is one of the critical parameters determining the sonoluminescence and the sonochemical activity at the studied conditions. Fig. 1 shows that [O_2] drops as the temperature increases. Under silent conditions the measured [O_2] values fit well with published data at atmospheric pressure [20]. In the presence of ultrasound the

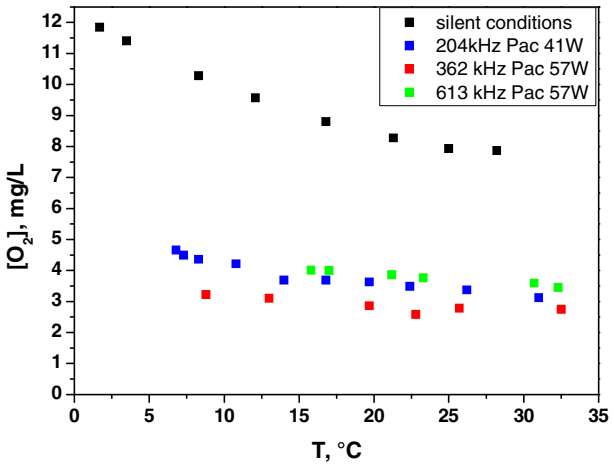

Fig. 1. Effect of temperature on the concentration of dissolved oxygen under silent conditions (◆) and at 204 kHz (P_{ac} = 41 W), 362 and 613 kHz (P_{ac} = 57 W) ultrasound (■). Bubbling of Ar/20%O_2 mixture at 80 mL min^{-1}, no mechanical stirring. The uncertainty on [O_2] measurements is of 5%.

oxygen content is strongly decreased. Degassing of liquids has been among the first effects of ultrasound known for decades [21]. The mechanism of this process involves bubble nucleation, their growth owing to the directed diffusion of dissolved gas to the bubbles, as described in detail by Eskin [22], their coalescence by the action of secondary Bjerknes force and finally their release owing to buoyancy of the bubbles from the liquids submitted to ultrasound. This phenomenon allows to reach a concentration of dissolved gases in sonicated liquids lower than in freestanding liquids at ambient pressure. In the presence of ultrasound bubble coalescence is strongly influenced by primary and secondary Bjerknes forces [23]. On the other hand, the bubble–bubble interactions also depend on the experimental conditions, such as ultrasonic frequency, acoustic power, presence of electrolytes and surfactants, etc [24,25]. Fig. 2 demonstrates that at 20 kHz an increase in P_{ac} improves ultrasonic degassing. The same tendency was observed at 362 and 613 kHz (P_{ac} = 43 and 57 W; the results are not shown).

Fig. 3 reveals that the efficiency of ultrasonic degassing, ED (mg W^{-1}), defined as $ED = \frac{[O_2]_\infty - [O_2]_{US}}{P_{ac}/V}$, where $[O_2]_\infty$ and $[O_2]_{US}$ are the concentrations of dissolved oxygen under silent conditions and ultrasound respectively (mg L^{-1}), P_{ac} is the absorbed acoustic power (W) and V is the volume of treated solution (L), is practically independent from ultrasonic frequency at the studied conditions (20 °C, P_{ac} = 40–43 W). Such a behavior can be attributed to several parameters of acoustic cavitation. First, a 20 kHz ultrasound produces a limited conical cavitation zone near the horn tip while high-frequency ultrasound yields a more diffuse, widely distributed zone of cavitation. This may be counterbalanced by much higher mixing efficiency at 20 kHz compared to high-frequency ultrasound. Second, the cavitation event occurs at a faster rate at higher ultrasonic frequency. Besides, the bubble volume sharply drops with ultrasonic frequency. Also the number of bubbles and the extent of coalescence are expected to be frequency-dependent. Finally, the superposition of all these effects provides a relative independence of degassing efficiency from ultrasonic frequency in the particular case of P_{ac} = 40–43 W and 20 °C. It is to be noted however that a different trend may be obtained in other conditions of e.g. acoustic power, since as shown in Fig. 2 the amount of dissolved oxygen strongly depends on the acoustic power.

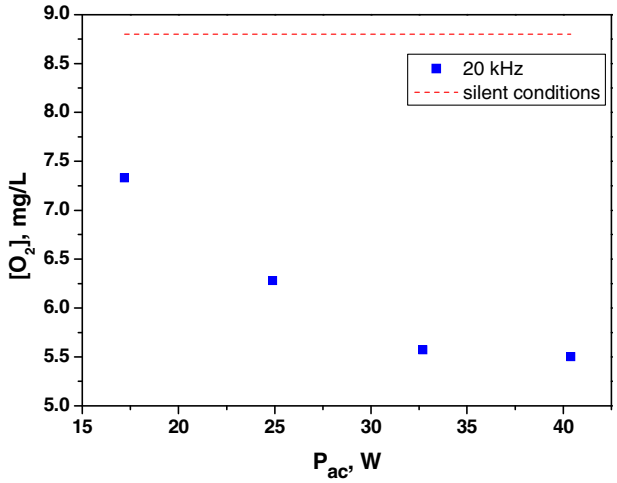

Fig. 2. Effect of acoustic power on the concentration of dissolved oxygen at 20 kHz ultrasound. Bubbling of Ar/20%O_2 mixture at 80 mL min^{-1}, no mechanical stirring, T = 12 °C. The dashed line indicates the concentration of dissolved oxygen under silent conditions.

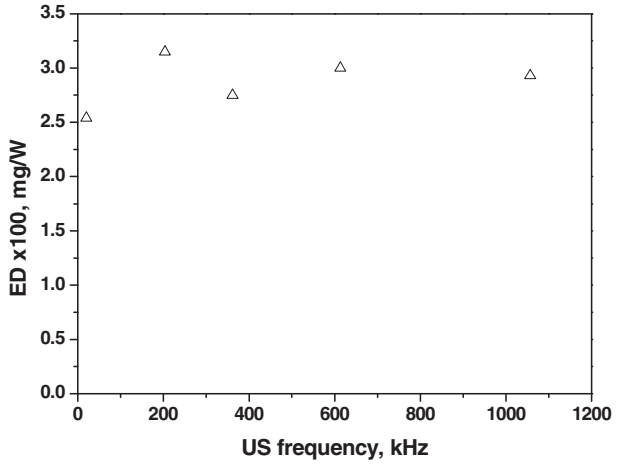

Fig. 3. Effect of ultrasonic frequency on oxygen degassing efficiency (uncertainty ±7%). Bubbling of Ar/20%O_2 mixture at 80 mL min^{-1}, 20 °C, no mechanical stirring, P_{ac} = 40–43 W.

3.2. Multibubble sonoluminescence in the presence of oxygen

Addition of oxygen to argon leads to surprisingly different impacts on MBSL spectra for low- and high-frequency ultrasound (Figs. 4 and 5). At 20 kHz, oxygen leads to a decrease in sonoluminescence in the whole studied range of concentrations. By contrast, at 362 kHz the use of Ar/20%O_2 gas mixture causes a 2-times increase in SL intensity in UVB (280–315 nm), near UV (300–400 nm) and visible (>400 nm) spectral range compared to pure Ar. The sharp drop in SL intensity at λ < 250 nm at high-frequency ultrasound in the presence of Ar/20%O_2 is most probably to be attributed to light absorption by hydrogen peroxide formed during water sonolysis. This observation presumes much higher H_2O_2 formation rate with Ar/20%O_2 mixture compared to pure Ar. Note here that in pure oxygen the sonoluminescence is quenched in the whole UV/Vis spectral range whatever the ultrasonic frequency.

Both gases, Ar and O_2, have very close solubilities in water (1.4 ± 0.1 mmol/kg) [20] so that no big difference in the bubble population is expected. Besides, the shapes of MBSL spectra collected in the presence of Ar/20%O_2 and Ar saturating gases are quite similar (Fig. 5) indicating that the strong enhancement of MBSL observed at 362 kHz for Ar/20%O_2 is related to a higher yield of light emitting species rather than to the generation of some new

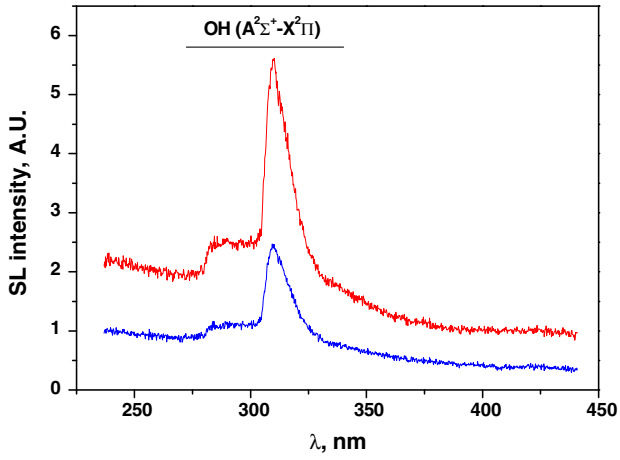

Fig. 4. MBSL spectra in water at 20 kHz in the presence of Ar (red line) and Ar/20%O_2 gas mixture (blue line). In pure O_2 the intensity of MBSL was negligibly low. P_{ac} = 17 W, T = 18 °C, gas bubbling at 80 mL min^{-1}. (For interpretation of the references to color in this figure legend, the reader is referred to the web version of this article.)

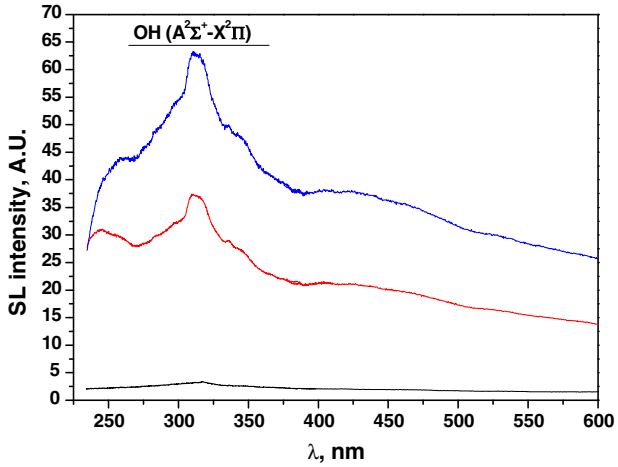

Fig. 5. MBSL spectra in water at 362 kHz in the presence of Ar (red line), Ar/20%O_2 gas mixture (blue line) and O_2 (black line). P_{ac} = 57 W, T = 13 °C, gas bubbling at 80 mL min^{-1}. (For interpretation of the references to color in this figure legend, the reader is referred to the web version of this article.)

excited species. In pure argon, the MBSL spectra of water are composed of the emission lines of excited OH· radicals and a featureless continuum which probably results from bremsstrahlung, H–OH· recombination and excited water molecules relaxation [18,19]. It is noteworthy that the emission from OH($A^2\Sigma^+$) state strongly contributes to total MBSL in water and that its emission intensity increases proportionally to that of the continuum when Ar is changed for Ar-20%O_2. Therefore, it is suggested that the intrabubble dissociation of O_2 molecules may significantly enhance the intensity of SL due to an increase in excited OH· radical production (see [26]):

$$H_2O\text{—}))) H + OH^{\cdot}\left(A^2\sum^{+}\right) \quad (1)$$

$$O_2^{\cdot}\text{—}))) 2O(^3P)(\Delta H = 5.2\text{eV mol}^{-1}) \quad [26] \quad (2)$$

$$O(^3P) + H_2O \rightarrow 2OH^{\cdot}\left(A^2\sum^{+}\right) \quad (3)$$

$$H + O(^3P) \rightarrow OH^{\cdot}\left(A^2\sum^{+}\right) \quad (4)$$

where the symbol "))" indicates a process occurring due to the acoustic collapse.

On the other hand, molecular oxygen is known to be a strong quencher of excited species [26]. For instance, effective quenching of single bubble sonoluminescence triggered by 20 kHz ultrasound in sulfuric acid has been reported recently in the presence of air [27]. Also it is known that oxygen is much more efficient in deactivating vibrationally excited OH($X^2\Pi$) hydroxyl radicals than nitrogen [28]. Therefore, one can suggest that the significant difference in the effect of O_2 on MBSL spectra of water at low- and high-frequency ultrasound be related to a higher degree of O_2 dissociation in the latter case. This hypothesis correlates with recent MBSL studies of OH· radicals in water saturated with noble gases which revealed the formation of a nonequilibrium plasma with stronger OH($A^2\Sigma^+$) vibrational excitation at higher ultrasonic frequency [19,29]. In terms of plasma chemistry higher vibrational excitation means higher electron temperature providing more efficient dissociation of thermodynamically stable molecules [30]. In pure oxygen, temperatures (in particular, electron temperature) reached at collapse are expected to be lower due to the higher heat conductivity of O_2 compared to Ar and the energy losses by vibrational excitation and dissociation of O_2 molecules. Besides, due to much higher intrabubble concentration of O_2 molecules, quenching by molecular oxygen gets predominant. These two arguments explain the much lower SL intensity measured in pure oxygen whatever the US frequency.

3.3. Kinetics of hydrogen peroxide formation

The sonochemical formation of H_2O_2 in Ar, Ar/20%O_2 and O_2 follows zero-order kinetics whatever the ultrasonic frequency. Fig. 6 demonstrates that the maximal value of H_2O_2 sonochemical formation rate, W(H_2O_2), is reached in Ar/20%O_2 gas mixture, in agreement with the data reported by other authors [5,10,12,15]. The significant acceleration of H_2O_2 formation rate at high-frequency ultrasound in the presence of Ar/20%O_2 gas mixture fits well with the sharp light absorption at λ < 250 nm in MBSL spectra shown in Fig. 5.

The increase of Ar/20%O_2 gas flow rate considerably enhances the sonochemical production of H_2O_2 at 362 kHz (Fig. 7). This is explained by a perfect correlation between W(H_2O_2) and the concentration of dissolved oxygen.

Furthermore, at high-frequency ultrasound the W(H_2O_2) values increase with the speed of mechanical stirring, ω, reaching a steady state at $\omega \geqslant 370$ rpm (Fig. 8). The beneficial effect of stirring is not (or not fully) explained by the increase in dissolved oxygen concentration (Fig. 7). Only a small decrease (4–15%) in the efficiency of degassing was observed at all four high frequencies for a stirring rate of 370 rpm. The higher W(H_2O_2) values can be related to more homogeneous distribution of the bubbles within the sonicated solution as it was reported by several authors [31,32]. At 204 kHz, visualization of the cavitation field performed with luminol using conventional procedure [33] clearly shows the disappearance of the standing wave pattern at 204 kHz and the enhancement of luminol chemiluminescence when mechanical stirring is applied (Fig. 9).

Fig. 10 demonstrates that in the presence of Ar/20%O_2 gas mixture and at 20 °C the maximal yield of H_2O_2 is observed at 204–362 kHz. In brief, one can say that 204–362 kHz ultrasound is approximately 10 times more efficient for sonochemical production of hydrogen peroxide compared to 20 kHz ultrasound. At 20 °C the degassing efficiency is approximately the same for 362–1057 kHz (Fig. 3) (at 204 kHz it is slightly higher due to the lower acoustic pressure used). So the dissolved oxygen content is not the parameter defining the optimal ultrasonic frequency range for H_2O_2 production here. The optimal ultrasonic frequency range for

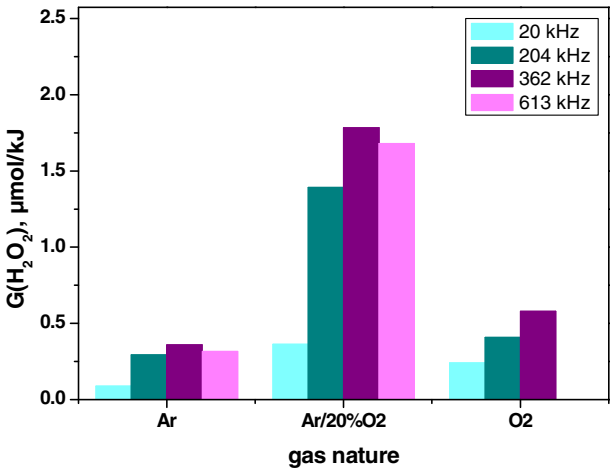

Fig. 6. Effect of oxygen concentration on the sonochemical yield of hydrogen peroxide. T = 20 °C, gas bubbling at 80 mL min^{-1}, no mechanical stirring. 20 kHz, P_{ac} = 33 W; 204 kHz, P_{ac} = 41 W; 362 kHz, P_{ac} = 43 W, 613 kHz, P_{ac} = 43 W.

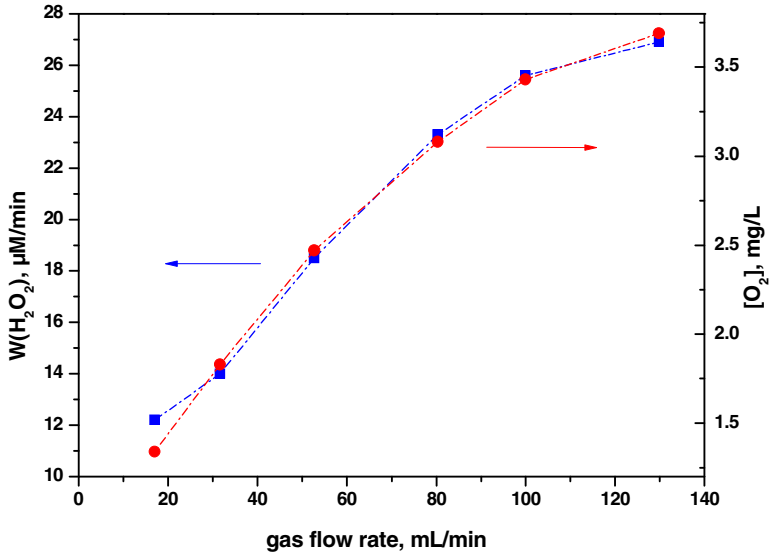

Fig. 7. Effect of Ar/20%O_2 gas flow rate on hydrogen peroxide formation rate and on the concentration of dissolved oxygen (362 kHz, P_{ac} = 73 W, 20 °C, no mechanical stirring).

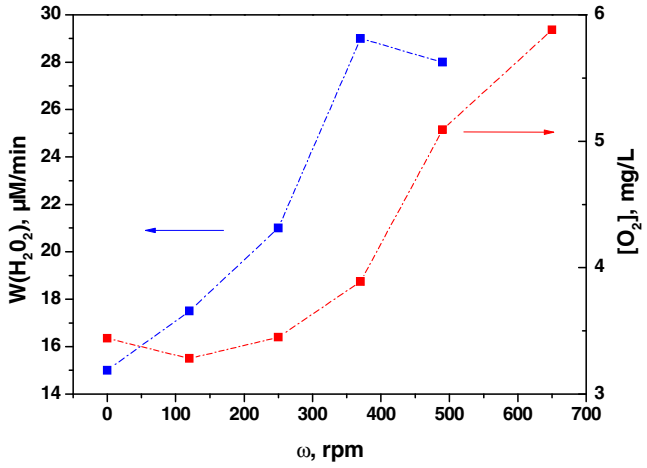

Fig. 8. Effect of mechanical stirring on hydrogen peroxide formation rate. f = 613 kHz, P_{ac} = 57 W, T = 40 °C, Ar/20%O_2 bubbling at 80 mL min^{-1}, and on the concentration of dissolved oxygen, f = 613 kHz, P_{ac} = 43 W, T = 15 °C, Ar/20%O_2 bubbling at 80 mL min^{-1}.

H_2O_2 production appears to be related to the intrabubble conditions (vibronic temperatures) and to the total sonochemically active volume (the concentration of active bubbles and their size distribution). Many parameters vary with the US frequency, that affect H_2O_2 production rate in different ways: (i) a faster rate of the cavitation events at high frequency, (ii) a dramatic decrease of the resonance bubble volume with ultrasonic frequency, (iii) a higher number of active bubbles at higher US frequency, (iv) more extreme conditions at high frequency with higher dissociation rate of O_2 molecules, and (v) longer collapse and larger bubble surface at low frequency, that allow more chemical reactions to take place at it. The optimal frequency for H_2O_2 formation is defined by the superposition of these five opposite phenomena.

An increase in bulk temperature to 40 °C causes the shift of $G(H_2O_2)$ maximal value to 613 kHz, however without any significant impact on H_2O_2 formation kinetics. By contrast, the total intensity of MBSL sharply decreases with bulk temperature. It was recently reported that the heating of argon-saturated water from 11 to 30 °C causes intensity of MBSL to decrease at least by a factor of 7 [19]. This phenomenon has been attributed to the quenching of excited species by water molecules inside the cavitation bubbles. Consequently, one can conclude that H_2O_2 is formed

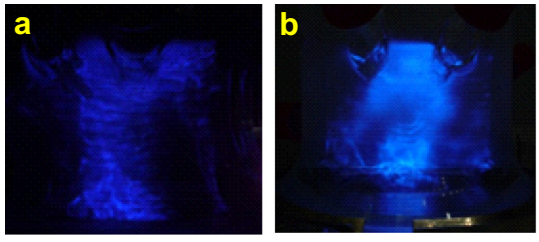

Fig. 9. Photographs of 0.01 M luminol solution (pH = 10.5 $NaHCO_3$) submitted to 204 kHz (P_{ac} = 32 W) ultrasound at 20 °C under Ar/20%O_2 bubbling (80 mL min^{-1}): (a) without stirring, (b) mechanical stirring at 370 rpm. The ultrasonic transducer was fitted at the bottom part of reactor. Exposition time of camera was 30 s.

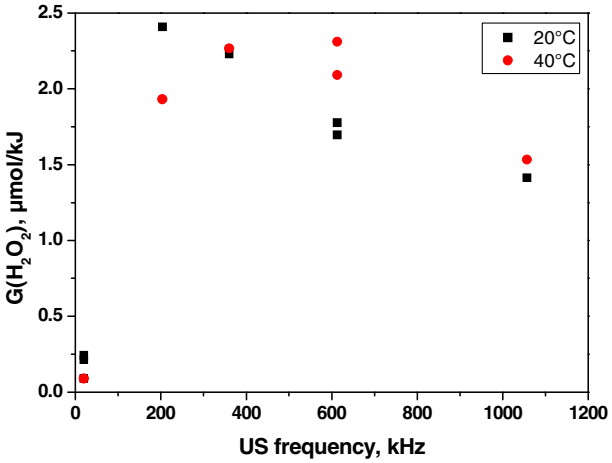

Fig. 10. Effect of ultrasonic frequency on the yield of H_2O_2. ■ 20 °C, ● 40 °C, Ar/20%O_2 bubbling at 80 mL min^{-1}, mechanical stirring at 370 rpm for high-frequency ultrasound, without stirring for 20 kHz ultrasound, acoustic power 33 W (20 kHz), 41 W (204 kHz), 57 W (362–1057 kHz). The energy consumption for mechanical agitation has been considered as insignificant.

Table 2
Hydrogen formation rate, $W(H_2)$, during the sonolysis of water in the presence of Ar and Ar/20%O_2. T = 20 °C, gas bubbling at 80 mL min^{-1}, no mechanical stirring.

$W(H_2)$, μM L^{-1} min^{-1}				
Gas	204 kHz P_{ac} = 41 W	362 kHz P_{ac} = 57 W	613 kHz P_{ac} = 57 W	1057 kHz P_{ac} = 56 W
Ar	2.7	3.6	4.0	3.5
Ar/20%O_2	0.26	0.34	0.26	0.05

Table 3
Comparison of hydrogen peroxide generation energy yields for sonochemical and plasma chemical processes in water at near room temperature.

Type of process	$G(H_2O_2)$, μmol kJ^{-1}
362 kHz ultrasound, Ar/20%O_2, 400 rpm	2.5[a]
362 kHz ultrasound, Ar, 400 rpm	0.5[a]
20 kHz ultrasound, Ar/20%O_2	0.4[a]
20 kHz ultrasound, Ar	0.06 [13]
Pulsed corona discharge, 60 Hz	12.6 [35]
AC capillary discharge	7.4 [35]
Radio frequency discharge	4.2 [35]

[a] This work.

mostly from non-excited radical species, via the recombination of OH· radicals at $X^2\Pi$ state or from HO_2 radicals:

$$OH^{\cdot}\left(A^2\sum{}^{+}\right) + H_2O \rightarrow OH^{\cdot}(X^2\Pi) + H_2O^{*}\ (\text{non-radiative quenching}) \quad (5)$$

$$2OH^{\cdot}(X^2\Pi) \rightarrow H_2O_2 \quad (6)$$

$$H + O_2 \rightarrow HO_2^{\cdot} \quad (7)$$

$$2HO_2^{\cdot} \rightarrow H_2O_2 + O_2 \quad (8)$$

Scavenging of H atoms by oxygen (reaction (7)) is confirmed by the sharp decrease in H_2 formation rate in Ar/20%O_2 compared to pure Ar (Table 2). According to published data [34] recombination of OH· radicals (reaction 6) occurs in the liquid shell surrounding the cavitation bubbles rather than inside the bubbles. The same reaction site can be suggested for reaction (8) since presumably hydrogen peroxide would not be stable under the drastic conditions generated in the gas phase of the collapsing bubbles.

Finally, it is useful to compare the efficiency of sonochemistry with other reagent-free techniques, such as plasma processes, considered as quite promising for waste water treatment [35]. Table 3 summarizes the $G(H_2O_2)$ values for different types of electric discharges in water as recently reviewed [35] and for sonochemistry as obtained in this work. In general, the yield of hydrogen peroxide in sonochemical process is lower than during electric discharge. Moreover, the sonolysis of water in the presence of pure argon at any ultrasonic frequency or in Ar/O_2 gas mixture at 20 kHz seems to be uncompetitive with plasma chemical processing. However, at optimal conditions (362 kHz, Ar/20%O_2, coupling of ultrasound with mechanical stirring) the sonochemical yield of hydrogen peroxide is comparable with that of an electric discharge. It is also important to point out that in contrast to sonochemistry the plasma chemical generation of OH· radicals is strongly affected by the conductivity of the treated solutions and the presence of suspensions [35,36]. For instance, according to reported data [36] the G(OH) value during pulsed discharge in water decreases more than 3.5 times when the conductivity increases from 100 to 500 μs cm^{-1}. Sonochemistry could provide a more reliable solution than plasma chemistry for the treatment of waste waters with high salt concentration or non-homogeneous wastes.

4. Conclusions

This study reveals a significant difference in MBSL at low- (20 kHz) and high- (362 kHz) frequency ultrasound in Ar–O_2 gas mixtures. At low frequency, molecular oxygen quenches sonoluminescence. At high-frequency ultrasound, the intensity of MBSL rises when the concentration of oxygen is increased to approximately 20%, but is almost totally quenched in pure oxygen. The enhancement of MBSL does not lead to any modification in the shape of sonoluminescence spectra. Such behavior can be explained by efficient dissociation of molecular oxygen during acoustic cavitation at high ultrasonic frequency. The secondary process of atomic oxygen with water provides higher yields of excited species (OH· radicals and water molecules). At 20 kHz ultrasound, O_2 dissociation is much weaker due to the lower vibronic temperatures reached inside the bubble. Therefore, at low ultrasonic frequency the quenching of excited species with molecular oxygen is a predominant process.

In contrast to MBSL, the maximal yield of H_2O_2 is observed at approximately 20% of O_2 in Ar–O_2 gas mixture whatever the frequency indicating that H_2O_2 is most probably formed from non-excited and, therefore, non-sonoluminescing species, such as OH· ($X^2\Pi$) and $HO_2^{\cdot}$ radicals. In pure oxygen, both sonoluminescence and sonochemistry are quenched, likely via rapid V–V process of $O_2(v)$–H_2O system well described for oxygen plasma [37] and because of the lower temperatures reached at collapse. In the presence of Ar/20%O_2 gas mixture and at 20 °C the maximal yield of H_2O_2 is observed at 204–362 kHz in agreement with previously published data. Interestingly, the increase of bulk temperature to 40 °C causes the shift of $G(H_2O_2)$ maximal value to 613 kHz, however without dramatic change in H_2O_2 formation rate. On the other hand, the intensity of MBSL sharply drops under heating of the sonicated solution up to 40 °C. Comparison of MBSL and sonochemistry allows to conclude that even non-sonoluminescing bubbles could preserve high sonochemical activity in the presence of Ar–O_2 gas mixture. This is in line with the previous conclusion about H_2O_2 formation from non-excited radical species. Coupling of high-frequency ultrasound with mechanical stirring or intensive carrier gas bubbling increases the yield in hydrogen peroxide. Visualization of the cavitation zone using chemiluminescence of luminol reveals that the beneficial effect of stirring is related to more homogeneous distribution of the bubbles within the sonicated medium. The effect of gas bubbling is mostly due to the solution saturation with oxygen. Finally, the obtained results allowed to conclude that at carefully selected experimental conditions, such as ultrasonic frequency, oxygen concentration, bulk temperature, gas bubbling and mechanical agitation, the sonochemical production of hydrogen peroxide seems to be competitive to plasma chemical technique.

Acknowledgements

L. Jouve acknowledges the support from Areva/Comurhex. Authors thank M. Virot and T. Martin for the help in some experiments.

References

[1] M.R. Hoffmann, I. Hua, R. Hochemer, Applications of ultrasonic irradiation for the degradation of chemical contaminants in water, Ultrason. Sonochem. 3 (1996) 163–172.
[2] Y.G. Adewuyi, Sonochemistry: environmental science and engineering applications, Ind. Eng. Chem. Res. 40 (2001) 4681–4715.
[3] Y.G. Adewuyi, Sonochemistry in environmental remediation. 1. Combinative and hybrid sonophotochemical oxidation processes for the treatment of pollutants in water, Environ. Sci. Technol. 39 (2005) 3409–3419.
[4] Y.G. Adewuyi, Sonochemistry in environmental remediation. 2. Heterogeneous sonophotocatalytic oxidation processes for the treatment of pollutants in water, Environ. Sci. Technol. 39 (2005) 8557–8570.
[5] C. Petrier, E. Combet, T. Mason, Oxygen-induced concurrent ultrasonic degradation of volatile and non-volatile aromatic compounds, Ultrason. Sonochem. 14 (2007) 117–121.
[6] Y.G. Adewuyi, B.A. Oyenekan, Optimization of a sonochemical process using a novel reactor and Taguchi statistical experimental design methodology, Ind. Eng. Chem. Res. 46 (2007) 411–420.
[7] P.R. Gogate, Treatment of wastewater streams containing phenolic compounds using hybrid techniques based on cavitation: a review of the current status and the way forward, Ultrason. Sonochem. 15 (2008) 1–15.
[8] N.N. Mahamuni, Y.G. Adewuyi, Advanced oxidation processes (AOPs) involving ultrasound for waste water treatment: a review with emphasis on cost estimation, Ultrason. Sonochem. 17 (2010) 990–1003.
[9] I. Grčić, S. Papić, N. Koprivanac, Sonochemical effectiveness factor (e_{US}) in the reactors for wastewater treatment sono-Fenton oxidation: novel considerations, Ultrason. Sonochem. 20 (2013) 1037–1045.
[10] C. Petrier, A. Jeunet, J.-L. Luche, G. Reverdy, Unexpected frequency effects on the rate of oxidative processes induced by ultrasound, J. Am. Chem. Soc. 114 (1992) 3148–3150.
[11] I. Hua, M.R. Hoffmann, Optimization of ultrasonic irradiation as an advanced oxidation technology, Environ. Sci. Technol. 31 (1997) 2237–2243.
[12] M.A. Beckett, I. Hua, Impact of ultrasonic frequency on aqueous sonoluminescence and sonochemistry, J. Phys. Chem. A 105 (2001) 3796–3802.
[13] N.M. Navarro, T. Chave, P. Pochon, I. Bisel, S.I. Nikitenko, Effect of ultrasonic frequency on the mechanism of formic acid sonolysis, J. Phys. Chem. B 115 (2011) 2024–2029.
[14] L. Milne, I. Stewart, D.H. Bremner, Comparison of hydroxyl radical formation in aqueous solutions at different ultrasound frequencies and powers using the salicylic acid dosimeter, Ultrason. Sonochem. 20 (2013) 984–989.
[15] E.J. Hart, A. Henglein, Free radical and free atom reactions in the sonolysis of aqueous iodide and formate solutions, J. Phys. Chem. 89 (1985) 4342–4347.
[16] C.-H. Fischer, E.J. Hart, A. Henglein, Ultrasonic irradiation of water in the presence of $^{18,18}O_2$: isotope exchange and isotopic distribution of H_2O_2, J. Phys. Chem. 90 (1986) 1954–1956.
[17] M. Zhou, N.S.M. Yusof, M. Ashokkumar, Correlation between sonochemistry and sonoluminescence at various frequencies, RSC Adv. 3 (2013) 9319–9324.
[18] R. Pflieger, H.-P. Brau, S.I. Nikitenko, Sonoluminescence from OH($C^2\Sigma^+$) and OH($A^2\Sigma^+$) radicals in water: evidence for plasma formation during multibubble cavitation, Chem. Eur. J. 16 (2010) 11801–11803.
[19] A.A. Ndiaye, R. Pflieger, B. Siboulet, J. Molina, J.-F. Dufreche, S.I. Nikitenko, Nonequilibrium vibrational excitation of OH radicals generated during multibubble cavitation in water, J. Phys. Chem. A 116 (2012) 4860–4867.
[20] E. Wilhelm, R. Battino, R.J. Wilcock, Low-pressure solubility of gases in liquid water, Chem. Rev. 77 (1977) 219–262.
[21] A.E. Crowford, Ultrasonic Engineering, Butterworths, London, UK, 1955.
[22] G.I. Eskin, Cavitation mechanism of ultrasonic melt degassing, Ultrason. Sonochem. 2 (1995) S137–S141.
[23] R. Mettin, I. Akhatov, U. Parlitz, C.D. Ohl, W. Lauterborn, Bjerknes forces between small cavitation bubbles in a strong acoustic field, Phys. Rev. E 56 (1997) 2924–2931.
[24] A. Brotchie, F. Grieser, M. Ashokkumar, Effect of power and frequency on bubble-size distributions in acoustic cavitation, Phys. Rev. Lett. 102 (2009) 084302.
[25] A. Brotchie, T. Statham, M. Zhou, L. Dharmarathne, F. Grieser, M. Ashokkumar, Acoustic bubble sizes, coalescence, and sonochemical activity in aqueous electrolyte solutions saturated with different gases, Langmuir 26 (2010) 12690–12695.
[26] T.G. Slanger, R.A. Copeland, Energetic oxygen in the upper atmosphere and the laboratory, Chem. Rev. 103 (2003) 4731–4765.
[27] D.J. Flannigan, K.S. Suslick, Plasma quenching by air during single bubble sonoluminescence, J. Phys. Chem. A 110 (2006) 9315–9318.
[28] L. D'Ottone, D. Bauer, P. Campuzano-Jost, M. Fardy, A.J. Hynes, Vibrational deactivation studies of OH $X^2\Pi$ (v = 1–5) by N_2 and O_2, Phys. Chem. Chem. Phys. 6 (2004) 4276–4282.
[29] A.A. Ndiaye, R. Pflieger, B. Siboulet, S.I. Nikitenko, The origin of isotope effects in sonoluminescence spectra of heavy and light water, Angew. Chem. Int. Ed. 52 (2013) 2478–2481.
[30] A. Fridman, Plasma Chemistry, Cambridge University Press, Cambridge, USA, 2008.
[31] S. Hatanaka, H. Mitome, K. Yasui, S. Hayashi, Multibubble sonoluminescence enhancement by fluid flow, Ultrasonics 44 (2006) e435–e438.
[32] T.J. Mason, J.P. Lorimer, Applied Sonochemistry. The Uses of Power Ultrasound in Chemistry and Processing, Wiley-VCH, Weinheim, Germany, 2002.
[33] T. Toru, K. Yasui, T. Kozuka, A. Towata, Y. Iida, Enhancement of sonochemical reaction rate by addition of micrometer-sized air bubbles, J. Phys. Chem. A 110 (2006) 10720–10724.
[34] S.I. Nikitenko, L. Veanult, Ph. Moisy, Scavenging of OH radicals produced from H_2O sonolysis with nitrate ions, Ultrason. Sonochem. 11 (2004) 139–142.
[35] B.R. Locke, K.-Y. Shih, Review of the methods to form hydrogen peroxide in electrical discharge plasma with liquid water, Plasma Sources Sci. Technol. 20 (2011) N034006.
[36] M. Sahni, B.R. Locke, The effects of reaction conditions on liquid-phase hydroxyl radical production in gas–liquid pulsed electrical discharge reactors, Plasma Process. Polym. 3 (2006) 668–681.
[37] R. Ono, Y. Teramoto, T. Oda, Vibrational temperature and vibrational relaxation of molecular oxygen in the afterglow of pulsed positive corona discharge, in: 29th International Conference on Phenomena in Ionized Gases, ICPIG, July 12–17 (2009) Cancun, Mexico.